

**High- $x$  structure function of the virtually free neutron**Wim Cosyn<sup>1,\*</sup> and Misak M. Sargsian<sup>2,†</sup><sup>1</sup>*Ghent University, 9000 Ghent, Belgium*<sup>2</sup>*Florida International University, Miami, Florida 33199, USA*

(Received 31 July 2015; revised manuscript received 17 April 2016; published 23 May 2016)

The pole extrapolation method is applied to the semi-inclusive inelastic electron scattering off the deuteron with tagged spectator protons to extract the high- $x$  structure function of the neutron. This approach is based on the extrapolation of the measured cross sections at different momenta of the spectator proton to the nonphysical pole of the bound neutron in the deuteron. The advantage of the method is in the possibility of suppression of the nuclear effects in a maximally model-independent way. The neutron structure functions obtained in this way demonstrate a surprising  $x$  dependence at  $x \geq 0.6$  and  $1.6 \leq Q^2 \leq 3.38 \text{ GeV}^2$ , indicating a possible rise of the neutron-to-proton structure functions ratio. If the observed rise is valid in the true deep inelastic region then it may indicate new dynamics in the generation of high- $x$  quarks in the nucleon. One such mechanism we discuss is the possible dominance of short-range isosinglet quark-quark correlations that can enhance the  $d$ -quark distribution in the proton.

DOI: [10.1103/PhysRevC.93.055205](https://doi.org/10.1103/PhysRevC.93.055205)**I. INTRODUCTION**

Detailed knowledge of the  $u$  and  $d$  quark densities at large Bjorken  $x$  is one of the important unresolved issues in the QCD structure of the nucleon. This structure is very sensitive to quark correlation dynamics at short distances [1]. The high- $x$  distribution is important also to Large Hadron Collider (LHC) physics, in which due to QCD evolution, the partons at very large virtualities are sensitive to the high- $x$  quark distributions measured at lower  $Q^2$ .

The extraction of the separate  $u$  and  $d$  quark distributions in the nucleon requires either the measurement of the deep inelastic scattering (DIS) structure function of the proton and neutron or weak interaction measurements off the proton in the charged current sector. Currently, the bulk of the data comes from the studies of inclusive electron DIS off the proton and deuteron, with the latter being used to extract the neutron structure functions. In this case, nuclear effects such as the relativistic motion of the bound nucleons and their medium modification in the deuteron become increasingly important at higher  $x$ , rendering the extracted neutron structure functions strongly model dependent (see, e.g., Refs. [2–4]).

One solution to the problem is to consider a new generation of experiments in which electron DIS off the deuteron is followed by the detection of a recoil proton [5,6], i.e.,

$$e + d \rightarrow e' + X + p. \quad (1)$$

Such processes are more complex due to the large final-state interactions (FSI) of the DIS products with the spectator proton at large momenta [7,8]. Their advantage, however, lies in the possibility of applying the pole extrapolation procedure [9,10] at small momenta of the proton, in which case all nuclear effects due to Fermi motion, FSI, and medium modification can be significantly suppressed in a practically model-independent way.

In Sec. II we introduce the general concept of pole extrapolation and explain why it is best suited for reactions involving a deuteron target. Section III presents the theoretical framework of tagged deep inelastic scattering, which is then used in Sec. IV to elaborate the pole extrapolation procedure for reaction (1). In Sec. V we present the details of the pole extrapolation applied to the recent Barely Off-shell Nucleon Structure (BONuS) data and our results for neutron structure function at large Bjorken  $x$ . In Secs. VI and VII we discuss the results and present the conclusions.

**II. GENERAL CONCEPT OF POLE EXTRAPOLATION**

The pole extrapolation was first suggested by Chew and Low [11] for probing the structure of so-called free  $\pi$  mesons or the neutron by studying (a)  $h + p \rightarrow h' + \pi + N_s$  and (b)  $h + p \rightarrow h' + n + \pi_s^+$  reactions. In these reactions,  $N_s$  and  $\pi_s^+$  can be considered as spectators to the underlying  $h + \pi \rightarrow h' + \pi$  and  $h + n \rightarrow h' + n$  subprocesses, in which  $h$  is an external probe. Their idea was that by extrapolating the invariant momentum transfer to the unphysical pole values of the bound particles ( $m_\pi$  and  $m_n$  in this case), it will be possible to extract the free cross sections of the underlying subprocesses.

The general concept of pole extrapolation can be seen if one considers a target  $A$  that consists of two bound constituents  $B$  and  $C$  in the reaction in which  $B$  is probed by a particle  $h$ , while the particle  $C$  emerges as a spectator. The impulse approximation (IA) (Fig. 1) amplitude of such process has a structure

$$M_{IA} = M^{h_1+B \rightarrow h_2+X} \frac{G(B)}{t - M_B^2} \chi_C^\dagger \Gamma^{A \rightarrow BC} \chi_A, \quad (2)$$

where  $\chi_A$  and  $\chi_C$  represent the wave functions of incoming composite particle  $A$  and outgoing spectator particle  $C$ . The vertex  $\Gamma^{A \rightarrow BC}$  characterizes the  $A \rightarrow BC$  transition and the propagator of bound particle  $B$  is described by  $\frac{G(B)}{t - M_B^2}$ , with  $t = (p_A - p_C)^2$ . As it follows from Eq. (2), the IA amplitude

\*wim.cosyn@ugent.be

†sargsian@fiu.edu

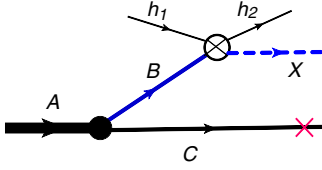


FIG. 1. IA contribution to  $h_1 + A \rightarrow h_2 + C + X$  reaction, with  $C$  acting as a spectator.

has a singularity in the nonphysical limit  $t \rightarrow M_B^2$ . The most important property which makes this singularity significant is the so-called loop theorem [9], according to which any other process beyond IA will not be singular due to a loop integration. Thus, even though non-IA terms can be large in the physical domain, they will be corrections in the  $t \rightarrow M_B^2$  limit.

The accuracy of the extrapolation depends on the magnitude of

$$l = m_B^2 - t_{\text{thr}}, \quad (3)$$

where  $t_{\text{thr}}$  is the threshold value for the physical domain.

For the reaction (a)  $t_{\text{thr}} = 0$ ,  $l = m_\pi^2 \approx 0.02 \text{ GeV}^2$ , and for (b)  $t_{\text{thr}} = (m_N - m_\pi)^2$ ,  $l = 2m_N m_\pi - m_\pi^2 \approx 0.24 \text{ GeV}^2$ . While  $l$  is small for reaction (a), the problem is that the pole is positive and  $t < 0$ , so the extrapolation requires a crossing of the  $t = 0$  point which makes the result very sensitive to small variations in the method of extrapolation. For reaction (b), even if one stays in positive domain of  $t$ ,  $l$  is quite large, introducing ambiguities in the analytic form of the pole extrapolation.

It was observed in Ref. [9] that pole extrapolation is well suited for reactions (1) for which  $A \equiv d, B \equiv n$  and  $C \equiv p$ . In this case  $t_{\text{thr}} = (M_d - m_p)^2$  and the variable  $l$  is very small,  $l = 2m_n |\epsilon_b| - \epsilon_b^2 \approx 0.004 \text{ GeV}^2$ , with deuteron binding energy  $\epsilon_b \approx 2.2 \text{ MeV}$ . Another advantage is the positiveness of  $t = (p_p - p_D)^2 > 0$ ; thus no zero crossing issues arise. These features make the extrapolation procedure in reactions (1) very precise. Because of this, the pole extrapolation in processes involving the deuteron is considered as a main method in extraction of different neutron structure functions at future electron-light-ion colliders [12].

### III. THEORETICAL FRAMEWORK OF TAGGED SPECTATOR DIS

From the above discussion, it follows that reaction (1) is well suited for the extraction of neutron structure functions using the pole extrapolation method. The reaction (1) can be described through four nuclear structure functions  $F_{L,T,TT,TT}^{\text{SI}}$ , which depend on  $Q^2, x, \alpha_s, \mathbf{p}_{s\perp}$ , where  $\mathbf{p}_s$  is the proton momentum and  $\alpha_s = 2 \frac{E_s - p_s^z}{E_D - p_D^z}$  is the light-cone momentum fraction of the deuteron carried by the spectator proton normalized such that  $\alpha_s + \alpha_i = 2$  ( $\alpha_i$  is the equivalent quantity for the struck neutron). The virtual photon has energy  $\nu$  and momentum  $\mathbf{q}, Q^2 = \mathbf{q}^2 - \nu^2$ , Bjorken  $x = \frac{Q^2}{2m_N \nu}$ , and  $\hat{z} \parallel \mathbf{q}$ . Considering the proton integrated over the azimuthal angle  $\phi$  in the laboratory

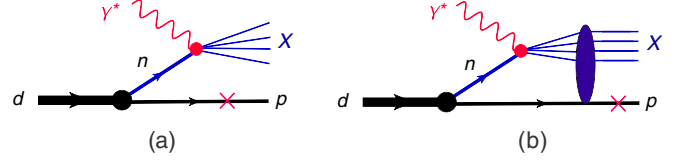


FIG. 2. IA (a) and FSI (b) contributions to reaction (1).

frame, one obtains

$$\begin{aligned} \frac{d\sigma}{dx dQ^2 d^3 p_s / E_s} &= \frac{4\pi \alpha_{\text{EM}}^2}{x Q^4} \left( 1 - y - \frac{x^2 y^2 m_N^2}{Q^2} \right) \left[ F_{2D}^{\text{SI}}(Q^2, x, \alpha_s, \mathbf{p}_{s\perp}) \right. \\ &\quad \left. + \frac{2\nu \tan^2 \frac{\theta}{2}}{m_N} F_{1D}^{\text{SI}}(Q^2, x, \alpha_s, \mathbf{p}_{s\perp}) \right], \quad (4) \end{aligned}$$

where  $F_{2D}^{\text{SI}} = F_L^{\text{SI}} + \frac{Q^2}{2q^2} \frac{\nu}{m_N} F_T^{\text{SI}}$ ,  $F_{1D}^{\text{SI}} = \frac{F_T^{\text{SI}}}{2}$ , and  $y = \frac{\nu}{E_e}$ .

The calculation of Eq. (4) at  $p_s < 700 \text{ MeV}/c$  and  $x > 0.1$  is based on the assumption [5,7,9] that the scattering proceeds through the interaction of the virtual photon off one of the bound nucleons in the deuteron. Two main diagrams contribute: IA [Fig. 2(a)] and final-state interaction (FSI) diagrams [Fig. 2(b)], where the latter accounts for the rescattering of the recoil nucleon off the products of DIS. While the calculation of the IA term requires the knowledge of the deuteron wave function and the treatment of the off-shellness of the bound nucleon, the FSI term requires in addition the modeling of the deep inelastic rescattering dynamics. In Ref. [7], we developed a theoretical model for the calculation of the FSI contribution based on the extension of the generalized eikonal approximation (GEA) model [13,14] to the DIS domain (see also Ref. [15]). The off-shell effects were treated within the virtual nucleon approximation (VNA), which works reasonably well for up to  $\sim 500 \text{ MeV}/c$  of spectator nucleon momenta, as our previous experience in the quasielastic regime shows [16–18].

The calculations based on this approach [7] demonstrated a good agreement with the first data from Jefferson Laboratory (JLab) [19] (referred to as *DeepS* data) in the  $x > 0.3$  and  $p_s \geq 300 \text{ MeV}/c$  region, describing all the major features of the angular and momentum distributions. The conclusion from these comparisons was that at  $x > 0.3$ , the FSI is dominated by the so-called compound DIS products scattering off the recoil nucleon, which can be characterized by a diffractive scattering amplitude. The wide kinematical range of Ref. [19] allowed us to extract the deep inelastic FSI cross sections as a function of  $x$  and  $Q^2$ . The success in the description of the data [19] motivated us to apply the pole extrapolation to extract the neutron structure functions  $F_{2n}(x, Q^2)$ . The data, however, were taken at large recoil momenta  $p_s \geq 300 \text{ MeV}/c$ , rendering large uncertainties in the pole extrapolation procedure [10]. More recently, a dedicated tagged DIS experiment was completed by the BONuS Collaboration [20,21], where the recoil proton was measured at unprecedentedly small momenta of  $78 \text{ MeV}/c$ . These data are the first in their kind for which the pole

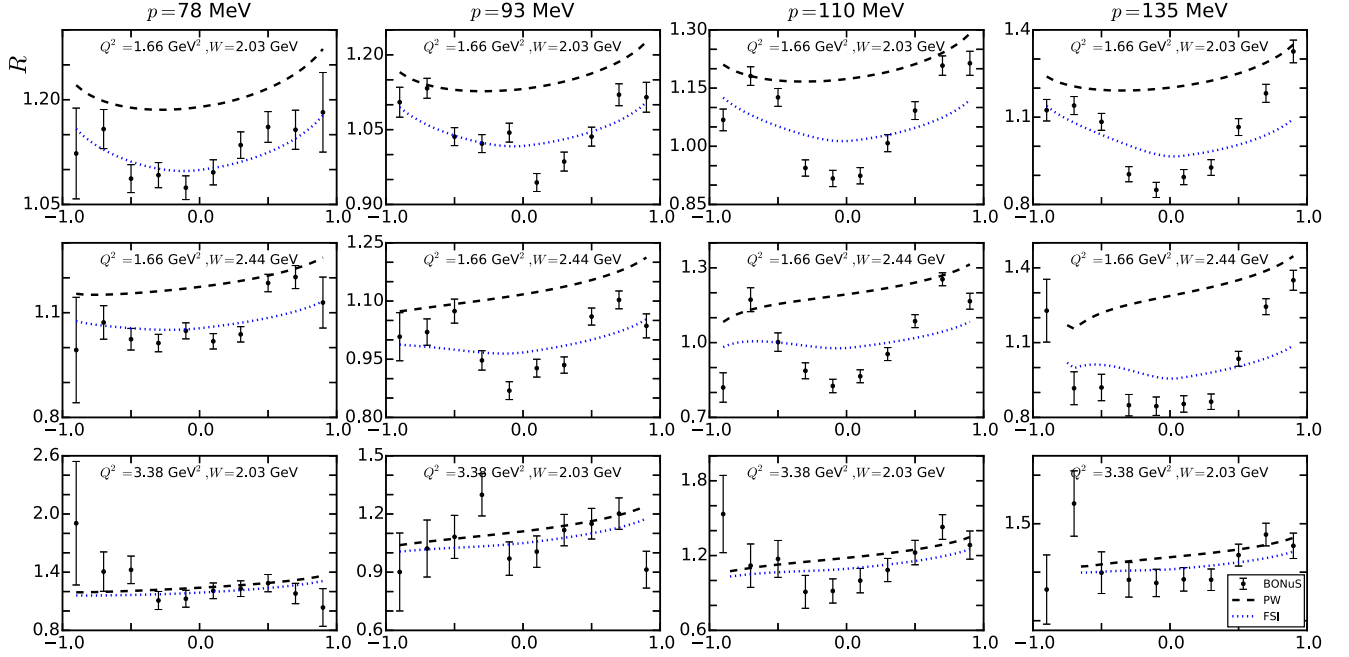


FIG. 3. Ratio  $R$  of the BONUS data to a plane-wave model (see Ref. [21] for details) as a function of spectator  $\cos \theta_s$ , compared to our VNA IA (black dashed curve) and FSI (dotted blue curve) calculation for  $E_{\text{beam}} = 4.23$  GeV. An overall normalization factor was fitted for each  $p_s$  value in the model to the FSI calculation; see text for details. The IA calculation is shown using the same normalization factor.

extrapolation can be performed with a higher degree of accuracy.

#### IV. POLE EXTRAPOLATION OF TAGGED DIS PROCESSES

The pole extrapolation in (1) uses the fact the IA amplitude of Fig. 2(a) [similar to Eq. (2)] can be expressed as [9]

$$M_{IA}^\mu = \langle X | J_{EM}^\mu(Q^2, x) | n \bar{u}(p_d - p_s) \bar{u}(p_s) \rangle \times \frac{\Gamma_{d \rightarrow pn} \chi_d}{|\epsilon_b| (M_d + m_n - m_s) + 2M_d T_s}, \quad (5)$$

where  $T_s$  is the kinetic energy of the spectator proton. In Eq. (5) the pole is associated with negative kinetic energy of the spectator at  $T_s^{\text{pole}} = -\frac{|\epsilon_b|}{2} (1 + \frac{m_n - m_p}{M_d}) \approx -\frac{|\epsilon_b|}{2}$ . While the above IA amplitude diverges at  $T_s \rightarrow T_s^{\text{pole}}$ , the FSI amplitude is finite due to an extra loop integration. In the  $T_s \rightarrow T_s^{\text{pole}}$  limit [9],

$$M_{FSI}^\mu \rightarrow J_{EM}^\mu(Q^2, x) \bar{u}(p_d - p_s) \bar{u}(p_s) \Gamma_{d \rightarrow pn} \chi_d \times \int \frac{d^3 k}{2k^2 (2\pi)^3} \frac{A_{FSI}(k)}{2(m_N + T_s^{\text{pole}} - k_0)}, \quad (6)$$

where  $k_0 = E_s - \sqrt{m_p^2 + (p_s - k)^2}$  and  $A_{FSI}$  is the diffractive-like amplitude of the rescattering of DIS products off the spectator proton. Equation (6) is finite at the pole as compared to the singular behavior of IA term. This result is the essence of the so-called loop theorem [9].

The pole extrapolation procedure for the extraction of  $F_{2n}$  consists of multiplying the measured structure function,  $F_{2D}^{\text{SI,EXP}}$  [Eq. (4)] by the factor  $I(\alpha_s, \mathbf{p}_{s\perp}, t)$  [9], which cancels

the singularity of the IA amplitude and is normalized such that

$$F_{2n}^{\text{extr}}(Q^2, x, t) = I(\alpha_s, \mathbf{p}_{s\perp}, t) F_{2D}^{\text{SI,EXP}}(Q^2, x, \alpha_s, \mathbf{p}_{s\perp}) \quad (7)$$

approaches the free  $F_{2n}(Q^2, x, t)$  in the  $t \rightarrow m_n^2$  limit with FSI effects being diminished.

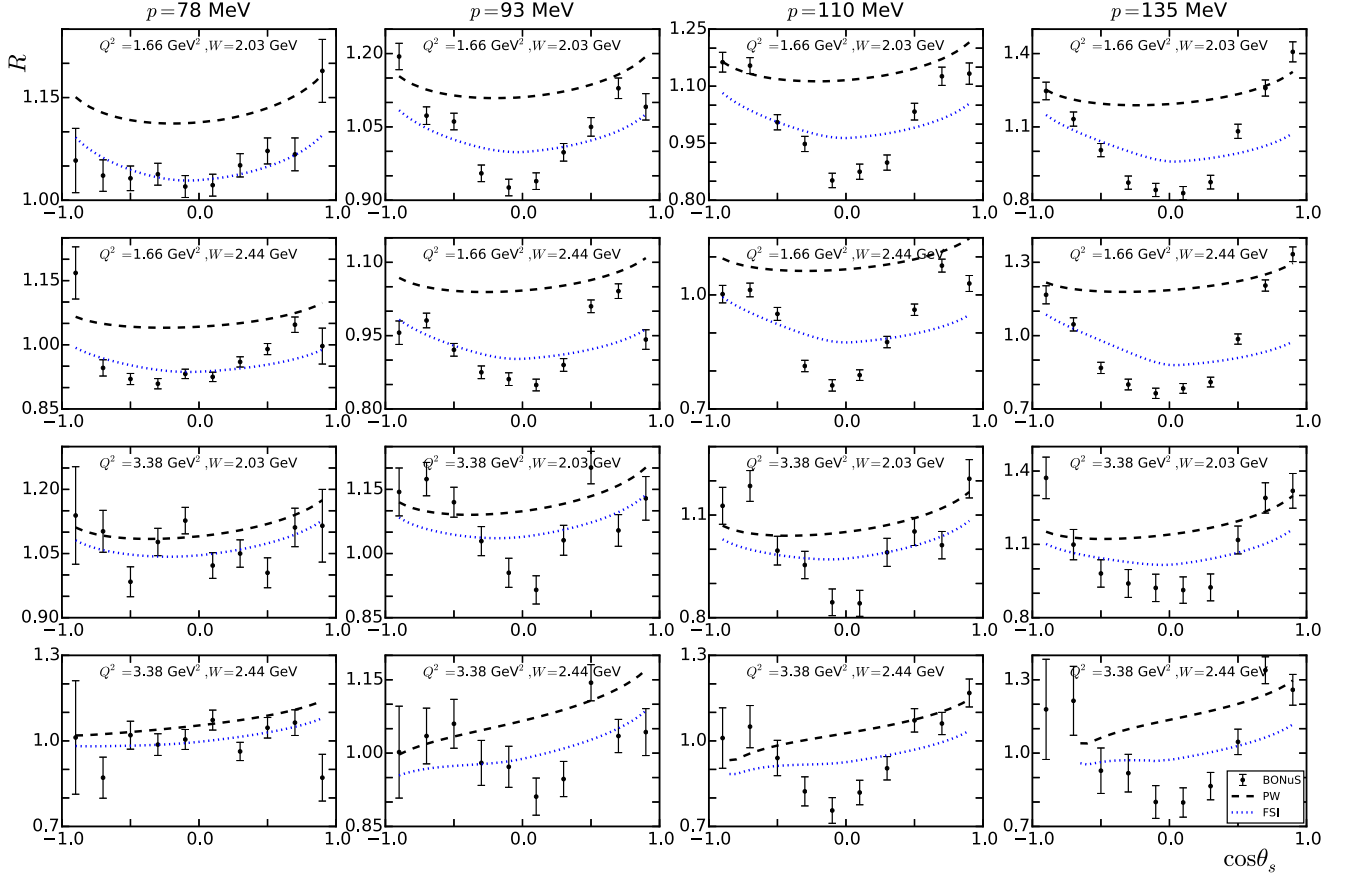
#### V. POLE EXTRAPOLATION OF THE BONUS DATA

We applied the above described method to the BONUS data [20,21], which covers the kinematic range of  $0.93 \leq Q^2 \leq 3.38$  GeV<sup>2</sup> and invariant mass of the DIS products  $1.18 \leq W \leq 2.44$  GeV. The spectator proton was detected at  $p_s = 77.5, 92.5, 110, 135$  MeV/c, covering a wide angular range of  $-0.9 \leq \cos \theta_s \leq 0.9$ .

##### A. Renormalization procedure

The problem in implementing the pole extrapolation procedure directly was in the fact that in the BONUS experiment different spectator momenta were measured at different and poorly known efficiencies. In the BONUS analysis this issue was solved by normalizing the data for each  $p_s$  bin at  $\cos \theta_s \leq -0.2$  to an IA model [21]. For our analysis, we chose to renormalize the data to the VNA calculation [7] discussed in Sec. III, since it also contains the FSI effects (referred in the text as VNA FSI). For these calculations we used the parametrization of the FSI amplitude ( $A_{FSI}$ ) obtained from the comparisons with the *DeepS* data [19].

The BONUS data are presented as ratios  $R$  of the BONUS data to the specific plane-wave impulse approximation (BONUS IA) model discussed in Ref. [21]. The overall normalization of the data was fitted for each spectator momentum setting for two values of initial beam energies. To obtain the

FIG. 4. As Fig. 3 but for  $E_{\text{beam}} = 5.27$  GeV.

absolute cross sections (required for the pole extrapolation), we first multiplied the reported  $R$  ratios by the BONuS IA calculation. Then these cross sections have been fitted to our VNA FSI calculations for each experimental  $p_s$  setting and initial beam energy in the range of  $x < 0.5$  where neutron DIS structure functions are sufficiently well known and have small contributions from nuclear effects. The results are presented in Figs. 3 and 4. For each column in these figures, corresponding to a fixed spectator momentum  $p_s$  and initial electron energy  $E_{\text{beam}}$ , one overall normalization factor was obtained. The values of the normalization factors with their errors are shown in Table I. The quoted normalization parameters are relative to

TABLE I. Normalization factors obtained by fitting the BONuS data to our VNA model calculations including FSI.

$E_{\text{beam}}$ (GeV)	$p_s$ (MeV)	Norm. factor	Error	$\chi^2/\text{dof}$
4.23	77.5	1.316	0.036	2.39
	92.5	1.279	0.033	4.61
	110	1.378	0.041	11.1
	135	1.494	0.055	10.2
5.27	77.5	1.176	0.025	6.54
	92.5	1.203	0.026	12.4
	110	1.244	0.031	15.7
	135	1.417	0.047	20.8

the BONuS normalization values. Since BONuS obtained their absolute cross sections by fitting their IA model, we basically renormalized the BONuS cross sections to take into account the FSI effects. As was mentioned above, the parameters of FSI are fixed from the analysis of the only existing (*DeepS*) experiment of reaction (1) [19]. This experiment covered larger values of the spectator proton momentum ( $\geq 300$  MeV/c), which was good for the extraction of FSI parameters. However, the restricted kinematics of *DeepS* measurements prevent us from obtaining the sufficiently detailed FSI parametrization to be able to describe the shape of the ratio  $R$  in a more refined way in the  $\cos(\theta_s) \approx 0$  region dominated by the FSI of produced resonances. Further refinements of FSI parameters will allow us to address the more detailed structure of the cross section dominated by resonance production.

In Figs. 3 and 4 we also compare the results of VNA calculation within the impulse approximation (referred to as VNA IA) with the same normalization factors of Table I. These calculations indicate that the FSI effects are not negligible and they increase with the spectator momentum  $p_s$ .

To estimate the errors in the normalization factors we investigated their dependence on several VNA FSI model ingredients: The first is the choice of the deuteron wave function. To estimate the wave function uncertainty we used a selection of different deuteron wave functions, AV18 [22], CDBonn [23], Paris [24], and WJC1 [25], resulting in  $<0.5\%$  variations. The uncertainty in the parametrization of the FSI

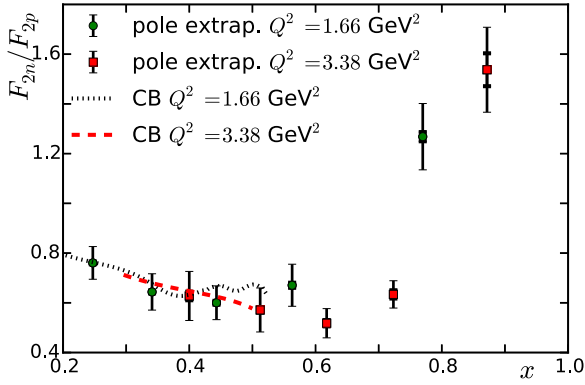


FIG. 5.  $F_{2n}$  to  $F_{2p}$  ratio obtained using the pole extrapolation applied to the renormalized BONuS data. Systematic errors are depicted as open error bars. The dotted black and dashed red curves show the ratio obtained with  $F_{2n}$  parametrization of Ref. [26]. The  $F_{2p}$  values are estimated using the fit of Ref. [27].

amplitude obtained in Ref. [7] resulted in 2–3% variations. Finally, in the VNA calculation at  $x < 0.5$ , we used the neutron structure functions parametrization from Ref. [26], whose average accuracy in this region is  $\sim 3\%$ .

As follows from Table I, our fitting procedure yielded rather large values for  $\chi^2/\text{dof}$ . This is mainly due to small values of the statistical errors in BONuS data, which were taken into account in the fitting procedure. Inclusion of the systematic errors of BONuS data will significantly reduce the magnitude of  $\chi^2/\text{dof}$ . However, we did not include the latter into the fit since it was unclear whether these errors are uncorrelated. Finally, as a test that the renormalization procedure yielded valid results, we compared our extracted (by pole extrapolation method) neutron structure functions at  $x < 0.5$  with the data available from the analysis of inclusive  $d(e, e')X$  reactions [26]. Note that the inclusive  $d(e, e')X$  reactions at  $x < 0.5$  have small contribution from nuclear effects and neutron data in this kinematics can be considered rather reliable. As Fig. 5 shows, our results agree reasonably well with that of Ref. [26].

### B. Pole extrapolation in the $x > 0.5$ regions

The experimental uncertainties in the absolute cross section of the BONuS data depend only on the momenta of the spectator proton  $p_s$  at given  $E_{\text{beam}}$  and not on the range of the  $x$  being probed. Therefore, the normalization factors that we obtained for the  $x < 0.5$  region can be applied to the BONuS data set also in the  $x > 0.5$  region, where the neutron structure functions are not well constrained. In this way, we obtained the renormalization of the BONuS data set for the whole measured region of  $x$ . Using these renormalized data in the pole extrapolation procedure described in Sec. IV, we extracted the neutron structure functions for the whole range of the  $x$  covered by BONuS experiment.

The extracted  $F_{2n}$  for the largest two  $Q^2$  bins of the BONuS experiment are presented in Fig. 5 and Table II. These represent the weighted average of the extrapolated values taken over all

TABLE II.  $F_{2n}$  and its ratio to  $F_{2p}$  with statistical and systematic errors, obtained with the pole extrapolation method applied to the renormalized BONuS data.

$Q^2(\text{GeV}^2)$	$x$	$F_{2n}$	Stat.	Sys.	$\frac{F_{2n}}{F_{2p}}$	Stat.	Sys.
1.66	0.25	0.251	0.002	0.022	0.761	0.006	0.066
	0.34	0.181	0.002	0.020	0.644	0.006	0.073
	0.44	0.153	0.002	0.017	0.600	0.008	0.067
	0.56	0.118	0.002	0.015	0.671	0.010	0.084
	0.77	0.090	0.001	0.009	1.268	0.019	0.132
3.38	0.40	0.147	0.004	0.023	0.628	0.017	0.10
	0.51	0.091	0.002	0.014	0.571	0.010	0.089
	0.62	0.061	0.001	0.007	0.518	0.013	0.057
	0.72	0.046	0.001	0.004	0.634	0.017	0.052
	0.87	0.030	0.001	0.003	1.54	0.066	0.158

$\theta_s$  bins. The final statistical errors are similar to those of the BONuS data averaged over backward  $\theta_s$  [20].

Our procedure of renormalization and pole extrapolation rendered systematic errors, which are presented (as open error bars) in Fig. 5. To estimate the systematic errors in the extracted  $F_{2n}$  values, we took into account statistical and systematic errors of the BONuS non-normalized cross sections as well as errors in the estimation of the renormalization coefficients of Table I.

To estimate the final systematic errors in the  $F_{2n}$  which are extracted in the pole extrapolation, we carried out a Monte Carlo simulation where each of the inputs in the pole extrapolation (BONuS un-normalized cross sections, renormalization coefficients, and the uncertainty in the factor  $I(\alpha_s, p_{s\perp}, t)$  due to the choice of the particular deuteron wave function) are distributed randomly in the Gaussian form with a width corresponding to their estimated errors. With such randomly distributed input values the pole extrapolation is carried out. The widths of the distribution of the extracted  $F_{2n}$  values are taken as an estimate for the systematic errors in our procedure. These are the systematic errors quoted in Table II. Note that in the future experiments [28] these systematic errors can be largely reduced by achieving more reliable absolute measurements of the data.

## VI. DISCUSSION OF THE RESULTS

The most important advantage of the pole extrapolation method is that the extracted neutron structure functions are free from Fermi motion and nuclear medium modification effects, which are the main and unresolved issues in high- $x$  extractions in inclusive DIS off the deuteron. Our results for  $F_{2n}/F_{2p}$  at  $x < 0.5$  are in fair agreement with the neutron structure functions extracted from the analysis of the inclusive data where no significant nuclear effects are expected. However, our results exhibit a few surprises at larger  $x$  (Fig. 5). First, at  $x > 0.6$ ,  $F_{2n}$  is larger than the one extracted in inclusive DIS. Note, however, that Fermi effect uncertainties in inclusive DIS analyses [4] still allow the values obtained in Fig. 5. The second interesting property of our results is the weak slope of the  $F_{2n}/F_{2p}$  ratio with increasing  $x$ , even indicating a possible upward turn of the ratio at  $x \gtrsim 0.7$ . The upward turn

is observed also in the  $d(e,e')X$  analysis [29] for up to  $x = 0.7$ , in which the medium modification effects in the deuteron are estimated using the observed correlation between nuclear EMC and short-range correlation effects.

Our analysis was applied to the data beyond  $x = 0.7$  and the intriguing result is that the tendency of the  $F_{2n}/F_{2p}$  ratio to increase continues. It is worth mentioning that the extracted slope of  $F_{2n}/F_{2p}$  is nearly insensitive to our normalization procedure. Due to sub-DIS values of  $W$  ( $\approx 1.18$  GeV) corresponding to the highest  $x$  values in Fig. 5 one cannot directly relate the rise of  $F_{2n}/F_{2p}$  to underlying properties of the  $u$ - and  $d$ -quark distributions at  $x \rightarrow 1$ . At these  $W$  such a rise is related to the  $F_{2n}$  of the  $\Delta$  production. Thus the relation to the properties of quark distributions can be made only based on duality arguments. It is worth mentioning that the recent duality paper [30] analyzing the same BONuS data concluded that the  $\Delta$  resonance contributes to the duality, within 20–30% accuracy.

If one assumes, however, that the observed  $F_{2n}/F_{2p}$  rise will persist in the true DIS region then it is intriguing that such a rise can be an indication of the existence of an isosinglet  $qq$  short-range correlations (SRCs) in the nucleon at  $x \rightarrow 1$ . Such a correlation will result in the same momentum-sharing effect, which is observed recently in asymmetric nuclei in the  $NN$  SRC region [31,32]. According to this observation, the SRC between unlike components in the asymmetric two-Fermi system will result in the small component's dominance in the correlation region such that

$$f_1 n_1(p) \approx f_2 n_2(p), \quad (8)$$

where  $f_i$  are the fractions of the components and  $n_i(p)$  the high momentum distributions normalized to unity. If such a  $qq$  SRC would be present in the nucleon, then the above equation will

translate to

$$u(x) \approx d(x) \quad (9)$$

at  $x \rightarrow 1$ , since the valence  $u$  and  $d$  quarks are normalized to their respective fractions. Such a relation will result in the rise of the  $F_{2n}/F_{2p}$  ratio in the region of  $x$  in which the  $qq$  correlations are dominant. Note that the possible dominance of isosinglet  $ud$  SRCs is consistent with the flavor decomposition of neutron and proton form factors in the large  $Q^2$  region [33].

## VII. CONCLUSION AND OUTLOOK:

For the first time the pole extrapolation procedure is used to extract  $F_{2n}$  from semi-inclusive scattering from the deuteron with a tagged recoil proton. The extracted results are free from Fermi and medium modification effects. They indicate a possible inversion of the decrease of the  $F_{2n}/F_{2p}$  ratios at large  $x$ . If such an increase would be observed in the true DIS region, it suggests the dominance of a short-range isosinglet  $ud$  correlations, which will result in the momentum sharing effects predicted for asymmetric two-component Fermi systems in which a short interaction takes place between unlike components.

## ACKNOWLEDGMENTS

We are thankful to O. Hen, S. Kuhn, E. Piasezky S. Tkachenko, M. Strikman, and Ch. Weiss for helpful discussions. The work is supported by Research Foundation Flanders and U.S. DOE grant under Contract No. DE-FG02-01ER41172. The computational resources used in this work were provided by Ghent University, the Hercules Foundation, and the Flemish government. We are thankful also to the Jefferson Lab theory group for support and hospitality, where part of the research has been conducted.

- 
- [1] R. Feynman, *Photon Hadron Interactions* (Westview Press, Boulder, CO, 1998).
  - [2] L. L. Frankfurt and M. I. Strikman, *Phys. Rep.* **160**, 235 (1988).
  - [3] W. Melnitchouk and A. W. Thomas, *Phys. Lett. B* **377**, 11 (1996).
  - [4] J. Arrington, J. G. Rubin, and W. Melnitchouk, *Phys. Rev. Lett.* **108**, 252001 (2012).
  - [5] W. Melnitchouk, M. Sargsian, and M. I. Strikman, *Z. Phys. A* **359**, 99 (1997).
  - [6] M. M. Sargsian *et al.*, *J. Phys. G* **29**, R1 (2003).
  - [7] W. Cosyn and M. Sargsian, *Phys. Rev. C* **84**, 014601 (2011).
  - [8] C. Ciofidegli Atti and L. P. Kaptari, *Phys. Rev. C* **83**, 044602 (2011).
  - [9] M. Sargsian and M. Strikman, *Phys. Lett. B* **639**, 223 (2006).
  - [10] W. Cosyn, *AIP Conf. Proc.* **1369**, 121 (2011).
  - [11] G. F. Chew and F. E. Low, *Phys. Rev.* **113**, 1640 (1959).
  - [12] W. Cosyn *et al.*, *J. Phys. Conf. Ser.* **543**, 012007 (2014).
  - [13] L. L. Frankfurt, M. M. Sargsian, and M. I. Strikman, *Phys. Rev. C* **56**, 1124 (1997).
  - [14] M. M. Sargsian, *Int. J. Mod. Phys. E* **10**, 405 (2001).
  - [15] W. Cosyn, W. Melnitchouk, and M. Sargsian, *Phys. Rev. C* **89**, 014612 (2014).
  - [16] M. M. Sargsian, *Phys. Rev. C* **82**, 014612 (2010).
  - [17] W. Boeglin and M. Sargsian, *Int. J. Mod. Phys. E* **24**, 1530003 (2015).
  - [18] W. U. Boeglin *et al.* (Hall A Collaboration), *Phys. Rev. Lett.* **107**, 262501 (2011).
  - [19] A. V. Klimenko *et al.* (CLAS Collaboration), *Phys. Rev. C* **73**, 035212 (2006).
  - [20] N. Baillie *et al.*, *Phys. Rev. Lett.* **108**, 142001 (2012); **108**, 199902 (2012).
  - [21] S. Tkachenko *et al.*, *Phys. Rev. C* **89**, 045206 (2014); **90**, 059901 (2014).
  - [22] R. B. Wiringa, V. G. J. Stoks, and R. Schiavilla, *Phys. Rev. C* **51**, 38 (1995).
  - [23] R. Machleidt, *Phys. Rev. C* **63**, 024001 (2001).
  - [24] M. Lacombe, B. Loiseau, J. M. Richard, R. Vinh Mau, J. Conte, P. Pires, and R. de Tourreil, *Phys. Rev. C* **21**, 861 (1980).
  - [25] F. Gross and A. Stadler, *Phys. Rev. C* **78**, 014005 (2008).
  - [26] P. E. Bosted and M. E. Christy, *Phys. Rev. C* **77**, 065206 (2008).

- [27] M. E. Christy and P. E. Bosted, *Phys. Rev. C* **81**, 055213 (2010).
- [28] S. Bueltmann *et al.*, E12-06-113, 2012 (unpublished).
- [29] L. B. Weinstein, E. Piasezky, D. W. Higinbotham, J. Gomez, O. Hen, and R. Shneor, *Phys. Rev. Lett.* **106**, 052301 (2011).
- [30] I. Niculescu *et al.*, *Phys. Rev. C* **91**, 055206 (2015).
- [31] M. M. Sargsian, *Phys. Rev. C* **89**, 034305 (2014).
- [32] O. Hen *et al.*, *Science* **346**, 614 (2014).
- [33] G. D. Cates, C. W. de Jager, S. Riordan, and B. Wojtsekhowski, *Phys. Rev. Lett.* **106**, 252003 (2011).